Chemical Engineering Science 69 (2012) 669–678

Contents lists available at SciVerse ScienceDirect

Chemical Engineering Science

journal homepage: www.elsevier.com/locate/ces

Dynamic modeling of combustion in a BioGrate furnace: The effect of operation parameters on biomass firing

Alexandre Boriouchkine *, Alexey Zakharov, Sirkka-Liisa Jämsä-Jounela

Aalto University, School of Chemical Technology, Department of Biotechnology and Chemical Technology, Process Automation Research Group, P.O. Box 16100, 00076 Aalto, Finland

ARTICLE INFO

Article history:
Received 1 February 2011
Received in revised form
28 October 2011
Accepted 21 November 2011
Available online 28 November 2011

Keywords:
BioGrate boiler
Renewable energy system
Grate firing of biomass
Power generation
Dynamic modeling
Conservative finite difference method

ABSTRACT

The development of efficient operation and control of a biomass boiler requires extensive knowledge of the combustion process inside the boiler furnace However, it is not possible to obtain the required knowledge through process measurements because the high temperatures and aggressive environment inside the furnace prevent taking accurate sensor readings. Instead, the process can be studied with the help of mathematical modeling. This paper describes dynamic modeling of bed combustion in a BioGrate boiler furnace. The developed dynamic model is heterogeneous, including solid and gas phases and corresponding reactions. The model is used for process phenomena investigation; the results are presented and discussed.

1. Introduction

Legislation supporting sustainable development is forcing industry to increase the share of electricity produced from renewable fuel. Consequently, the combustion of biomass is increasingly drawing the attention of the industry. However, the utilization of renewable energy sources poses several challenges. The challenges are mainly the result of significant variations in the quality of the fuels used. Biomass fuel quality depends mostly on the origin of the material and its processing technique. Moreover, different fuel batches can contain several different types of biomass. Consequently, each batch can consist of a wide range of fuels, whose varying properties cause large fluctuations during combustion and create challenges for process control and optimization. Extensive understanding of biomass combustion is therefore required to solve the challenges related to the process. Mathematical modeling can be used to acquire such knowledge (Jämsä-Jounela, 2007).

One of the most recently developed successful processes that use wood waste as fuel is based on the BioGrate boiler technology developed by MW Biopower. This technology was developed especially for the combustion of fuel with high moisture content, for example, wood chips. It is therefore important to study, among other effects of fuel properties, the effect of moisture content on the process behavior, and it is important to further optimize the process to ensure the maximal energy production rate. Wood combustion is however a very complex process, involving several tightly coupled chemical reactions and phase changes. Furthermore, the operational conditions of the furnace greatly affect the yields of chemicals produced during the combustion process, for example, fractions of tars, gases, and char. Moreover, not only the yields of chemicals differ under different combustion conditions but also their reactivity in succeeding reactions. As a result of such complexity, optimization of boiler operation requires a detailed process model.

The most recent publications on the modeling of solid fuel combustion on a grate concentrate on the combustion of either straw or municipal waste, including biomass. Shin and Choi (2000) have developed a one-dimensional model of waste incineration to better understand the phenomena occurring inside a municipal solid waste (MSW) incinerator. Van der Lans et al. (2000) have developed a two-dimensional, homogeneous model of the straw combustion process to optimize its design and operation parameters. Goh et al. (2001) have constructed a model of grate combustion of municipal solid waste in order to study the process, since efficient incinerator design requires extensive knowledge of the combustion process. Later, Yang et al. (2002) developed a 2-D model of an MSW incinerator, which was then verified using experimental data obtained from a pot reactor. Kær (2005) has developed a one-dimensional model to describe the fixed-bed combustion of straw and using the walking grate concept extended to cover the moving bed of a straw bed. Similarly, Zhou et al. (2005) assume insignificant horizontal temperature gradients in order to simplify to one dimension the thermal conversion model of a straw boiler furnace.

This paper describes the development of a mechanistic model of a BioGrate furnace. The aim was to construct a dynamic model

* Corresponding author. Tel.: +358 9 470 23178; fax: +358 9 470 23854.
E-mail addresses: alexandre.boriouchkine@aalto.fi (A. Boriouchkine), zakharov@cc.hut.fi (A. Zakharov), sirkka-l@tkk.fi (S.-L. Jämsä-Jounela).

0009-2509/$ - see front matter © 2011 Elsevier Ltd. All rights reserved.
doi:10.1016/j.ces.2011.11.032

providing an insight into the chemical and physical phenomena occurring in the process. Moreover, in describing the fuel combustion, close attention was paid to the kinetics of reactions because many previous studies neglected the fact that reaction rate equations are only valid for the conditions at which they were defined. Specifically, the validity of the reaction rate equations used was evaluated under the operation conditions of the BioGrate boiler furnace. Furthermore, the newest available kinetic knowledge on char combustion and pyrolytic gas composition was utilized to describe wood combustion. This paper is organized as follows: Section 2 describes the power generation process in a BioGrate power plant, Section 3 presents the model and its aspects, Section 4 discusses the implementation details of the model, Section 5 presents the simulation results, and Section 6 summarizes the results of simulations.

2. Process description of a BioGrate power plant

A BioGrate furnace consists of the following functional main parts: a grate and a water-filled reservoir below the grate to collect the ash. The BioGrate furnace is surrounded by heat-insulating refractory brick walls (combustion chamber), which reflect the heat radiation back to the grate.

The grate consists of several ring zones. Half of these rings rotate, and the other half are fixed. Every second rotating ring rotates clockwise, and the others rotate counterclockwise. This helps spread the fuel evenly over the surface of the conical grate.

Fuel is fed from below into the center of the grate, where it quickly dries as a result of the heat radiation that is emitted by the combusting flue gas and reflected back to the grate by the brick grate walls. The dry fuel then proceeds to the outer ring of the grate, where pyrolysis, char gasification, and combustion occur. The ash and carbon residues fall off the edge of the grate into a water-filled ash pit. Fig. 1 is a sketch of a BioGrate furnace. More details can be found in Anon (2011).

The air required in the gasification and combustion reactions is fed into the grate through grate nozzles underneath the grate (primary air) and through nozzles in the grate walls (secondary air). In addition, in order to ensure clean combustion, additional air can be supplied through the nozzles located at the top of the grate (tertiary air). Burning produces heat, which is absorbed in several steps. First, the boiler walls, acting as an evaporator, absorb part of the energy retained in the flue gases. Next, part of the energy of the flue gases is transferred to superheaters. In the third phase, heat is transferred to a convective evaporator. Finally, economizers remove the remaining heat energy from the flue gases.

The operation principle of a BioGrate power plant is based on steam generation. As any other biopower plant, a BioGrate power plant comprises several parts, including a boiler, a turbine generator, a feed-water tank, a water treatment plant, and a flue-gas cleaning system. Solid fuel is fed into the furnace of the boiler, where it is combusted, generating heat and flue gases. The heat is used to produce steam. Flue gases contain fly ash, which comprises several harmful components. Before being emitted into the atmosphere, the flue gases are therefore subjected to a multistage cleaning procedure that removes fly ash.

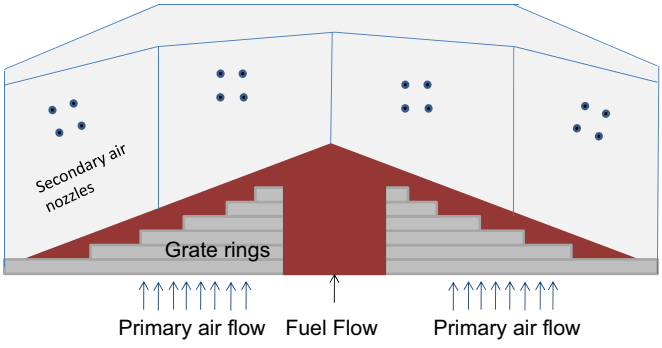

Fig. 1. BioGrate furnace.

The steam produced in the boiler is directed into a generator turbine, which converts the mechanical energy of steam into electricity. As steam performs mechanical work, its pressure decreases, after which it is used to heat utility streams, for example, of water (Kiameh, 2002). After steam has released enough energy, it condenses. The condensed steam is called condensate, which is fed into a feed-water tank along with pretreated feed water. Inside the tank, the liquid is heated with bled steam from the turbine. This procedure increases the energetic efficiency of the process (Kiameh, 2002).

3. Dynamic modeling

The dynamic model of a BioGrate furnace presented in this article aims to describe the combustion dynamics of biomass fuel inside the furnace. To provide acceptable accuracy, the model must consequently not only include the combustion kinetics, but also the shape of the furnace. The grate is conical and fuel is fed from the center, which means that the fuel spreads out on the grate as it moves outward. This enhances combustion by exposing more fuel to radiation reflected from the wall lining. As a result, the "walking grate" concept used to simulate combustion on sloping grates is modified to fit the BioGrate furnace.

The model of combustion kinetics is specifically selected to fit the operational conditions of the BioGrate. Furthermore, an experimental model is used to model the radiation distribution inside the furnace.

Despite the differences between the BioGrate furnace and those used in traditional combustion techniques, a biomass bed reacts in all these furnaces in a series of four different chemical reactions: drying, pyrolysis, char gasification, and char combustion (Peters and Bruch, 2001). Active drying starts when the temperature of a particle reaches the boiling point of water. Then high temperature initiates a pyrolysis reaction. The pyrolysis reaction produces gases, char, and tar. Gases are mainly composed of CO, CO_2, H_2, and C_1–C_3 hydrocarbons. Tar contains many organic components, such as levoglucosan, furfural, furan derivatives, and phenolic compounds (Di Blasi, 1996). Each reaction will be discussed in detail below.

3.1. Continuity equation models, their parameters and assumptions

3.1.1. Assumptions

Several assumptions are made in order to simplify the modeling work. The assumptions are listed in descending order of importance:

1. The system is assumed to be one dimensional, so the changes in temperature and mass along the horizontal axis are determined by the residence time. Visual observations of the actual combustion process reinforce this assumption, since the fuel appears to travel slowly along the grate in a pile without losing its form. Moreover, heat transfer inside the bed can be assumed to occur mostly in the vertical direction, since heat spreads towards cold areas in the direction of a normal to the bed surface. Since the height of the bed is significantly smaller than the length, the temperature gradient forms an almost 90° angle with respect to the horizontal axis.

2. Plug-flow gas assumption (Zhou et al., 2005). The gas phase is assumed to be ideal (Zhou et al., 2005; Kær, 2005)
3. The solid is assumed to be a porous material (Yang et al., 2003).
4. Diffusion in the gas phase is neglected since the effect of convection on the transportation of the gas is significantly greater (Peters and Bruch, 2001).
5. Pressure dynamics are ignored because the release of gaseous species is negligible in comparison with the primary air flow, and pressure evolution can therefore be neglected (Zhou et al., 2005).
6. Heat produced in char combustion is assumed to be retained in the solid phase (Zhou et al., 2005).
7. No volume reduction (shrinkage) occurs during drying, pyrolysis, and combustion (Di Blasi, 2009).
8. The temperature of the gas released from solids is the same as that of the solids (Zhou et al., 2005).
9. The temperature of solids in a discretized block is uniform (Zhou et al., 2005).
10. The heat capacity of the wood is assumed to be constant (Kær, 2005).
11. No heat loss.

Next, the simplified continuity equations are presented.

3.1.2. Solid phase continuity equation

The solid phase reactions consist of drying, pyrolysis, and char combustion:

$$\frac{\partial \rho_s}{\partial t} = -R_f \tag{1}$$

3.1.3. Energy continuity equation of the solid phase

The energy equation for the solid phase correlates heat conduction, heat exchange between phases, energy lost in drying and pyrolysis reactions, and energy gained in char combustion:

$$\frac{\partial T_s}{\partial t} C_s \rho_s = \frac{\partial}{\partial x}\left(k_{cond}\frac{\partial T_s}{\partial x}\right) + k_{conv} v_p (T_g - T_s) - R_{evap}\Delta H_{evap} - R_{pyr}\Delta H_{pyr} + R_{comb,C}\Delta H_{comb,C} - R_{gasi,CO_2}\Delta H_{gasi,CO_2} - R_{gasi,H_2O}\Delta H_{gasi,H_2O} \tag{2}$$

The radiation reflected from the grate walls to the fuel bed is described through boundary conditions defined as follows:

At the surface of the fuel bed, $x=a$

$$k_{cond}\frac{\partial T_s}{\partial x}\bigg|_{x=a} = I_{in} - e\sigma T_s^4 \tag{3}$$

To describe the energy flux I_{in}, an experimental model is used. The model is based on experimental data from a BioGrate boiler located in Trolhättan, Sweden.

$$k_{cond}\frac{\partial T_s}{\partial x}\bigg|_{x=0} = e\sigma T_s^4 \tag{4}$$

The heat conduction coefficient from the study of Yagi and Kunii (1957) is used to describe heat conduction in the bed:

$$\frac{k_e^0}{k_g} = \frac{\beta(1-\varepsilon)}{\gamma(k_g/k_s) + ((1)/((1/\phi) + d_p k_{rs}/k_g))} + \varepsilon\beta\frac{d_p k_{rv}}{k_g} \tag{5}$$

where the coefficient k_r describing the void-to-void heat conduction coefficient is presented in Eq. (6). Eq. (7) describes the solid surface-to-solid surface heat conduction coefficient, k_{rv}. The normal values of γ, φ, and β for cylinders and spheres, as well as for granules, are as follows (Yagi and Kunii, 1957):

$\gamma = 1, \quad \beta = 1, \quad$ and $\quad \varphi = 0.040.$

$$k_{rv} = \left(\frac{0.1952}{1+(\varepsilon/2(1-\varepsilon))}\frac{1-e}{e}\right)\left(\frac{T_s}{100}\right)^3 \tag{6}$$

$$k_{rs} = 0.1952\left(\frac{e}{1-e}\right)\left(\frac{T_s}{100}\right)^3 \tag{7}$$

Since wood is a porous material, inter-particular radiation must also be included in the effective heat transfer coefficient. According to Janssens and Douglas (2004), the radiative heat conduction coefficient inside the particle is

$$k_{s,rad} = \frac{4\varepsilon_{particle}\sigma {T_s}^3 d_{cavity}}{1-\varepsilon_{particle}} \tag{8}$$

$$d_{cavity} = 3.5\times 10^{-5}\sqrt{\varepsilon_{particle}} \tag{9}$$

During the combustion process, the porosity of the wood particle changes due to moisture evaporation, pyrolysis, and char combustion. Increasing porosity consequentially improves heat transfer inside the pore through heat radiation; therefore, porosity change is also included in the model. In Bryden and Hagge (2003), particle porosity evolution is accounted for with Eq. (10).

$$\varepsilon_{particle} = 1-(\rho_w+\rho_c)/1500-\rho_m/1000 \tag{10}$$

The effective heat conduction coefficient of the solid phase is (Janssens and Douglas, 2004):

$$k_{s.eff} = \varepsilon_{particle}k_{max} + (1-\varepsilon_{particle})k_{min} + k_{s,\ rad} \tag{11}$$

where k_{min} is given by Eq. (12) and k_{max} (W/(m K)) by Eqs. (12) and (13).

$$k_{min} = \frac{k_g k_{fiber}}{\varepsilon k_{fiber} + (1-\varepsilon)k_g} \tag{12}$$

$$k_{max} = \varepsilon k_g + (1-\varepsilon)k_{fiber} \tag{13}$$

where k_g is the heat conductivity of the gas inside the wood pores which assumed to be air.

According to Yagi and Kunii (1957), flowing fluid improves the heat conduction of the bed due to the effect of axial dispersion; therefore, the effective heat conduction coefficient becomes

$$k_{cond} = k_{cond,0} + \alpha\beta\cdot RePr \tag{14}$$

The geometrical constant is reported to typically take values between 0.1 and 0.13 (Yagi and Kunii, 1957). In the model, the average of $\alpha\beta = 0.115$ is used.

3.1.4. Gas phase continuity equation

Reacted solid components of wood are transferred to the gas phase; in addition, the gas phase continuity equation includes gas flow. Gas phase continuity equation is defined as follows:

$$\frac{\partial}{\partial t}(\rho_f \varepsilon_b Y_i) - \frac{\partial}{\partial x}(v_f \rho_f \varepsilon_b Y_i) = R_i \tag{15}$$

3.1.5. Energy continuity equation of the gas phase

Assuming no heat loss will occur, the energy continuity equation can be denoted as follows:

$$\frac{\partial h_f}{\partial t}\rho_f = -\frac{\partial}{\partial x}(\varepsilon_b v_f h_f) - k_{conv} v_p (T_g - T_s) + R_{comb,CO}\Delta H_{comb,CO} + R_{comb,H_2}\Delta H_{comb,H_2} \tag{16}$$

3.2. Chemical reactions in the model

The thermal decomposition of wood comprises three main chemical reactions: drying, pyrolysis, and char gasification with char combustion. In general, the chemical reactions can be described using experimental or semi-experimental models.

However, since Arrhenius dependence equations are simple to use and accurate, they have been used in this work.

3.2.1. Moisture evaporation

Commonly, fuels used in combustion processes contain moisture. Depending on the type of fuel, a fuel particle can contain various amounts of moisture. According to Thunman et al. (2004), fuel particles can contain up to 60 wt% of moisture with the char residue being as low as 10 wt% of the wet wood. Water can be bound to the structure of a wood particle or can reside in its pores.

Di Blasi et al. (2003) presented a simple yet accurate model to describe drying kinetics in updraft gasifiers, which, similarly to the BioGrate furnace, utilize countercurrent combustion conditions:

$$R_{evap} = 5.6 \times 10^8 \ \exp(-88[\mathrm{kJ/mol}]/\mathcal{R}/T_s)\rho_{Water} \quad (17)$$

3.2.2. Pyrolysis

After a particle has dried, the next reaction that occurs is pyrolysis. In pyrolysis, a dry wood particle is decomposed into tar, volatile organic components, and char. However, the fractions of tar, gas, and char found in the product yield heavily depend on the reaction conditions of the combustion process.

Alves and Figueiredo (1989) have presented a mathematical model of wet wood pyrolysis. The simulation results of this model were experimentally validated in the temperature range of 298–780 °C with a wet pine cylinder having the radius of 18.5 mm, with the water content being 45–49 wt%. The experimental and simulated results agreed. In the model, pyrolytic components are assumed to be cellulose and hemicellulose, since other components form less than 9% of the total wood mass (Alves and Figueiredo, 1989). However, these 9% were included in the mass fraction of hemicellulose, since these components and hemicellulose have the same reaction enthalpy and reaction rates of comparable magnitude. Cellulose constitutes 50 wt% of dry wood, while hemicellulose and other pyrolytic components 28 wt%. Furthermore, since devolatilization of cellulose is an endothermic reaction, the overall pyrolysis is also endothermic. Table 1 presents the reaction enthalpies of each pyrolytic component.

Cellulose reacts according to the following reaction rate equation (Alves and Figueiredo, 1989):

$$R_{devol,cel} = 2 \times 10^9 \ \exp(-146 \ [\mathrm{kJ/mol}]/\mathcal{R}/T_s)\rho_{cel} \quad (18)$$

Hemicellulose is reported to react according to the following reaction rate equation (Alves and Figueiredo, 1989):

$$R_{devol,Hemi} = 7 \times 10^4 \ \exp(-83[\mathrm{kJ/mol}]/\mathcal{R}/T_s)\rho_{Hemi} \quad (19)$$

3.2.3. Combustion of pyrolytic gases

The yield of pyrolytic gases is around 85 wt% under the operation conditions of a BioGrate furnace, for gasifying pyrolysis is the dominant pyrolysis mode under these conditions. This means that a significant amount of the energy used by the boiler comes from the combustion of gases, which indicates that the combustion of pyrolytic gases is the most important energy source. However, the composition of the gaseous products of pyrolysis reported in the study of Dupont et al. (2009) suggests that carbon monoxide has the highest concentration in the pyrolytic gas, while the fraction of other combustible gases remains under 10 wt%.

Table 1
Parameter values for pyrolysis reactions (Alves and Figueiredo, 1989).

Component	Enthalpy of reaction (kJ/kg)
Cellulose	322
Hemicellulose	−233

In the presence of water steam and oxygen, carbon monoxide is known to follow the following rate equation (Babushok and Dakdancha, 1993):

$$R_{comb,CO} = 1.3 \times 10^{14} \ \exp(-125.5[\mathrm{kJ/mol}]/\mathcal{R}/T_g)\cdot C_{CO}\cdot C_{O_2}^{0.5}\cdot C_{H_2O}^{0.5} \quad (20)$$

Hydrogen is reported to react according to the following rate equation (Babushok and Dakdancha, 1993):

$$R_{comb,H_2O} = 2.96 \times 10^{11} \ \exp(-6900[\mathrm{K}]/T_g)\cdot C_{H_2}\cdot C_{O_2}^{0.92} \quad (21)$$

Reaction rate of ethylene (Babushok and Dakdancha, 1993):

$$R_{comb,C_2H_4} = 2 \times 10^{12} \ \exp(-126[\mathrm{kJ/mol}]/\mathcal{R}/T_g)\cdot C_{C_2H_4}^{0.1} C_{O_2}^{1.65} \quad (22)$$

Reaction rate of acetylene (Babushok and Dakdancha, 1993):

$$R_{comb,C_2H_2} = 6.5 \times 10^{12} \ \exp(-126[\mathrm{kJ/mol}]/\mathcal{R}/T_g)\cdot C_{C_2H_2}^{0.5} C_{O_2}^{1.25} \quad (23)$$

Reaction rate of methane (Babushok and Dakdancha, 1993):

$$R_{comb,CH_4} = 5.6 \times 10^{12} \ \exp(-103800[\mathrm{kJ/mol}]/\mathcal{R}/T_g)\cdot C_{CH_4} \quad (24)$$

3.2.4. Char conversion reactions

Char combustion in the model is accounted for with the model presented in Senneca (2007). This model is chosen here because it is valid over the temperature range 440–800 °C, which corresponds to the temperature of char combustion in the BioGrate furnace. In addition, the pyrolysis conditions of char particles that were used to obtain the model parameters are similar to the pyrolysis conditions inside the BioGrate. The reaction rate equation for gas combustion defined in Senneca (2007) is presented below:

$$R_{CO} = 0.9X \times 1.4 \times 10^5 \ \exp(-100[\mathrm{kJ/mol}]/\mathcal{R}/T_s)P_{O_2}^{0.9}\rho_C \quad (25)$$

The gasification reaction of char with carbon dioxide (Senneca, 2007):

$$R_{gasi,CO_2} = 1.1 \times 10^9 \ \exp(-260[\mathrm{kJ/mol}]/\mathcal{R}/T_s)P_{CO_2}^{0.64}(1-X) \times\sqrt{1-2\ \ln(1-X)}\rho_C \quad (26)$$

The gasification reaction of char with water steam can become significant in the case of a BioGrate furnace because the fuel used contains a large amount of moisture. As a result, the recirculation gas used to control the temperature of the furnace can contain a high amount of water steam, promoting char gasification reactions with gaseous water (Matsumoto et al., 2009):

$$R_{gasi,H_2O} = P_{H_2O}^{0.22} \times 9.99 \times 10^4 \ \exp(-136[\mathrm{kJ/mol}]/\mathcal{R}/T_s) \ (1-X)\sqrt{1-10\ \ln(1-X)}\rho_C \quad (27)$$

4. Implementation of the models and description of the testing environment

The model is implemented in the MATLAB environment, in which a set of finite difference methods (FDMs) is used to solve the continuity equations. The reason for utilizing FDM is that it is well studied and all its drawbacks and stability issues are known; as a result, its suitability for a particular task is easy to evaluate. The Crank–Nicolson method is utilized to solve the energy equation for the solid phase because it involves heat conduction, which is a cubic function of the temperature. As a result, even small differences in temperature between subsequent time steps can cause severe oscillations; it is therefore necessary to use a second-order method in time. In addition, the Crank-Nicolson

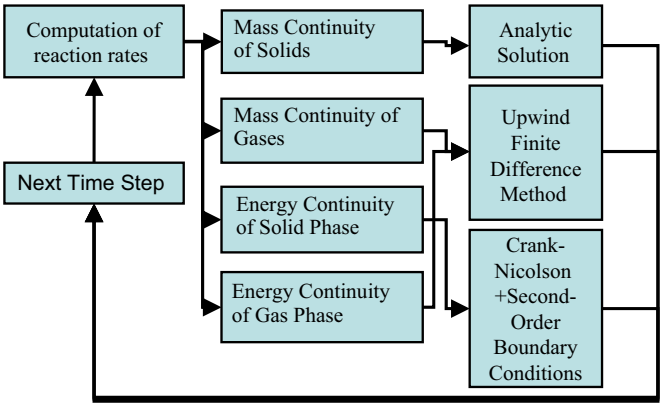

Fig. 2. Scheme of the solution algorithm.

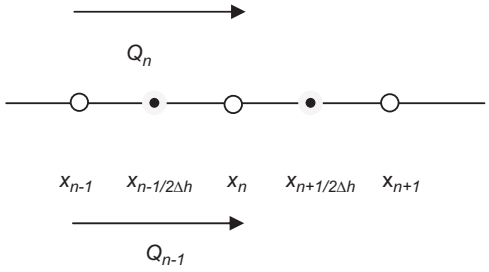

Fig. 3. Conservative modification of the Crank–Nicolson method.

method is coupled with second order boundary conditions to smooth out the steep temperature gradients at boundaries. The solution algorithm is presented in Fig. 2.

Furthermore, the Crank-Nicolson method is made conservative by considering the heat conduction term in the middle of a discretization interval instead of considering it at the discretization points themselves. The reason for this is that FDMs, in general, evaluate the heat flux leaving from point x_{n-1} towards point x_n, given in Eq.(28), and separately evaluate the heat flux arriving at point x_n from x_{n-1}, defined in Eq. (29). This property of FDMs can result in energy imbalance inside the system if the heat conduction coefficient itself depends on the temperature. Eqs. (28) and (29) show that these two fluxes are equal only when $k_{n-1}(\tau)$ and $k_n(\tau)$ are equal. Therefore, evaluating the heat conductivity coefficient as a function of the average temperatures of two subsequent discretization points ensures that k_{n-1} and k_n are equal and that energy is conserved (Ferziger and Peric, 2000). Fig. 3 illustrates the modification made to the numerical scheme.

$$Q_{n-1} = k_{n-1}\frac{(-u_n + u_{n-1})}{h} \tag{28}$$

$$Q_n = k_n\frac{(u_{n-1} - u_n)}{h} \tag{29}$$

5. Simulation results

This section presents the simulation results obtained with different fuel parameter values.

The operation of a boiler is based on the energy released from the combustion of fuel. Fuel combustion produces energy in the form of thermal radiation and the release of flue gases. However, the refractory grate wall directs radiation back to the fuel bed; in contrast, flue gases proceed to an evaporator, which produces steam. This makes flue gases, in addition to heat radiation, the most important energy source for the operation of the furnace. This paper therefore focuses on analyzing the operation of the furnace based on flue gas composition and mass flow as well as temperature. The simulation is conducted with pine wood chips as a fuel with a dry bed density of 150 kg/m^3. The bed porosity was assumed to be 0.5 while the ash content was fixed to be 1 wt% of the dry bed density. The effect of ash on heat conduction and convection is disregarded due to the small amount of ash compared with the total bed weight. Furthermore, when the density of a discretized volume has reached the density of ash, it is removed from the simulation. To make the visualization of the result presentation more convenient, the fuel layer height is fixed at the value of 10 cm despite the actual fuel layer height of the furnace being several times larger. This is due to fuel movement on the grate which lessens the reaction front depth for burning matter spreading to the larger area of the outer grate rings. The spatial step size used in simulations is 0.001 m, while the time step size is 1 s.

5.1. Fuel moisture content

Fuel moisture content is the most important quality property of fuel because excessive moisture in fuel induces large fluctuations in the power production of the boiler.

To investigate the fuel moisture effect on combustion, a simulation with four different moisture contents was conducted: 70, 60, 50, and 40 wt% of the total fuel weight. Primary air flow was fixed at 1 m^3/s, the particle size was assumed to be 35 mm, and the bed porosity was assumed to be 0.5. Fig. 4 depicts gas production rates for this simulation.

The simulation shows that fuels with 60 and 70 wt% moisture content exhibit a rapid increase in gas production after being subjected to the furnace temperature. Moreover, these fuels show a noticeably larger initial gas production rate than fuel with a lower moisture content. This is because the more moisture the fuel has, the quicker it will lose excess moisture and reach a stable drying rate. Nevertheless, after the top layer of the fuel bed has reached equilibrium in the drying rate, the gas production starts increasing, suggesting that fuel has ignited. Particularly, drier fuel ignites much more rapidly than wet fuel. Furthermore, the fuel with the highest moisture content, 70 wt%, seems not to burn properly, since it produces a rather slow increase in the gas production rate. After ignition, all fuels, however, achieve a relatively constant combustion front propagation rate: 0.03 kg/m^{2}s for the driest fuel and 0.02 kg/m^{2}s for the wettest one, with the values for other fuels in between these.

Later, the amount of released gas starts to decrease. The decrease is the result of the diminished contents of moisture and organic matter, for reaction rates are directly proportional to the concentration of reactants. The release of the flue gases continues to decrease until the fuel is dry. The dry fuel then undergoes a rapid devolatilization stage because energy is no longer consumed by drying. This causes a large spike in the gas production rate, which reaches 0.3 kg/m^{2}s for fuels with moisture contents of 40 and 50 wt% and reaches as high as 0.40 kg/m^{2}s in the case of the wettest fuel. The complete devolatilization of wood leaves only char. Char then participates in gasification and combustion reactions with carbon dioxide and oxygen. The devolatilization takes place throughout the entire grate, so there is time for char combustion on the grate before the char falls off the rotating grate rings. This allows a gasification reaction between char and water steam which produces hydrogen.

In addition to the combustion rate propagation, the moisture content also affects the how much gas is produced during combustion. The simulation shows that fuel with high moisture content tends to release less combustible gases because high moisture content prevents the temperature from rising, thereby

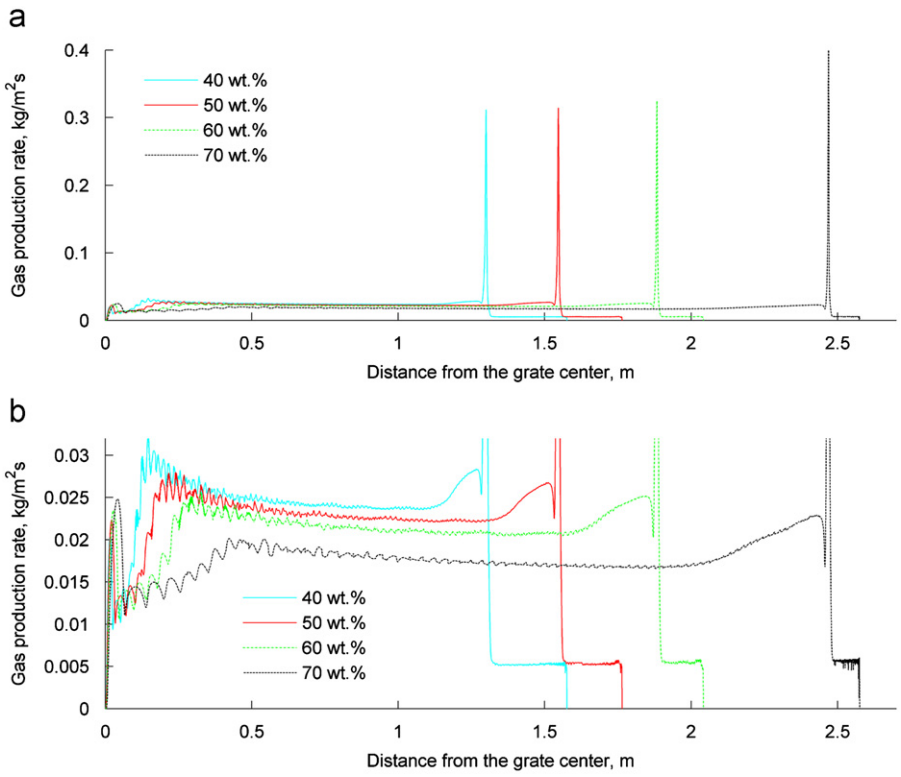

Fig. 4. (a) The overview of gas production rates of fuels with different moisture content and (b) the gas production rates, a close up.

delaying pyrolysis and limiting char combustion and gasification. Moreover, reactions that require high temperatures cannot start at all because the bed temperature does not rise above 500 °C. There is specifically no gasification at all of char with steam.

The results show that fuels with large moisture content burn cleaner because they have more oxygen available for the reactions; more specifically, they produce less carbon monoxide than carbon dioxide. Further, water steam forms almost 80% of the weight of the gas phase when the fuel moisture content is 70 wt%. Conversely, in the case of drier fuel, the weight fraction of carbon monoxide is almost twice as large as that of carbon dioxide. Fig. 5(a) and (b) presents the compositions of gases emitted from fuel beds with 40 and 70 wt% moisture content, respectively. In addition, dry fuel, while combusting, releases higher amounts of hydrogen, which is produced in the char gasification reaction with steam as well as in pyrolysis. In addition, the ignition of dry fuel is more apparent since a sharp rise in CO_2 can be observed. However, the CO_2 production from moist fuel increases gradually until the maximum is reached, after which it remains constant at a near-maximum level.

The composition of the flue gases consequently affects their temperature, for a large amount of energy is produced by the gas phase reactions. The temperature profiles of the gas phase clearly show that dry fuel produces considerably hotter gas than the fuel with the greatest moisture content. Specifically, the temperature of the flue gas leaving the fuel bed in the case of the fuel with a moisture content of 70 wt% has a temperature of 1000 °C, whereas, the corresponding temperature for fuel with a moisture content of 40 wt% is over 1500 °C.

The same effect on the fuel layer temperature profile is observed, for the drier fuel exhibits higher temperatures during combustion. More specifically, the temperature of the moist fuel does not rise above 500 °C, whereas the temperature of fuel with a moisture content of 40 wt% remains above 600 °C. Figs. 6 and 7 show the temperature profiles of fuels in the gas and solid phases and with different moisture contents. The combustion of drier fuel produces higher temperatures in both the gas and the solid phases, so it also affects the rates of chemical reactions involved in the biomass combustion. As a result, the oxygen content inside the fuel bed is also affected by the moisture.

The oxygen content profile reveals that the fuel with a moisture content of 70 wt% consumes almost no oxygen at all, whereas combustion of the drier fuels suffers from severe oxygen deficiency. This suggests that fuels with a low moisture content can be combusted with air flows greater than 1 m^3/s, whereas very moist fuel requires a much smaller air flow since excess air will only decrease the temperature of the bed.

In order to study the effect of a volumetric air flow, additional simulation was conducted using varying air flows while the fuel moisture content was fixed.

5.2. *Effect of air flow variation on fuel combustion*

The effect of air flow variation on fuel combustion was studied using the four different air flows of 0.5, 1, 2, and 4 m^3/s while the fuel moisture content was fixed at 50 wt%.

The simulation results show that the reaction front width decreases as the combustion air flow is increased. The decreased width is a consequence of increased oxygen flow since all available char can react. As a result, the mass of the fuel bed decreases more rapidly. Moreover, the increased air flow also cools the gas released from the bed because the air flow temperature is significantly lower than that of the flue gas. Increased air flow results in flue gas temperatures below 1000 °C with an air feed of 4 m^3/s, compared to above 1500 °C with an air flow of 1 m^3/s. Nevertheless, the difference in the mass degradation rates caused by the air flows of 1 and 4 m^3/s is insignificant, for the fuel reaches a point 1.8 m from the grate center with the air flow of 4 m^3/s, whereas the fuel is fully degraded at a point 1.6 m from the center with the air flow of

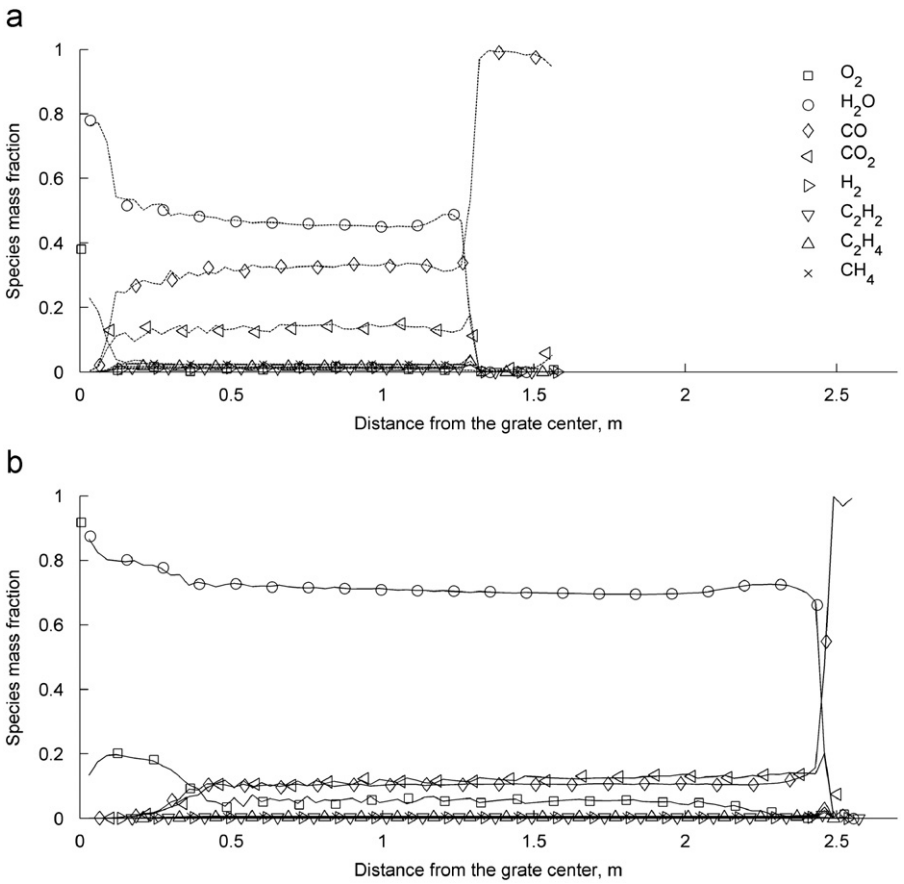

Fig. 5. The composition of flue gas originating from fuel with a moisture content of (a) 40 wt% and (b) 70 wt%.

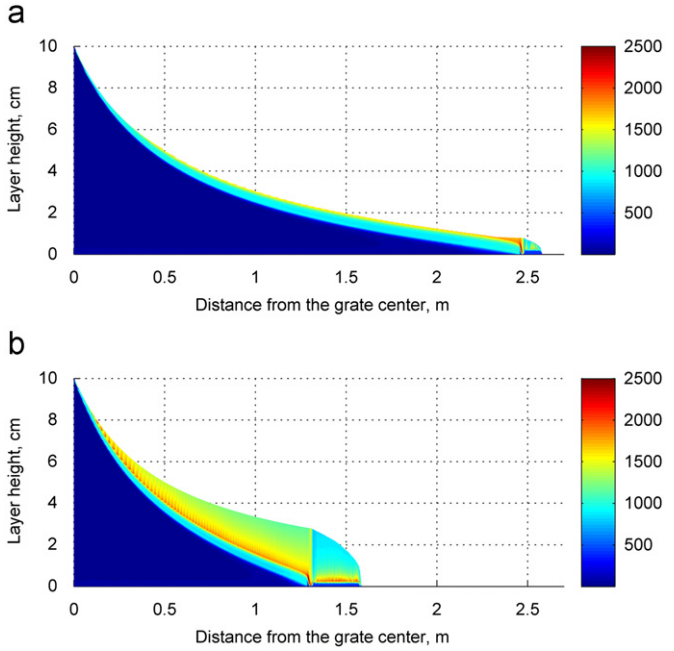

Fig. 6. Gas phase temperature profiles for fuels with (a) 70 wt% and (b) 40 wt% moisture contents with primary air flow of 1 m^3/s.

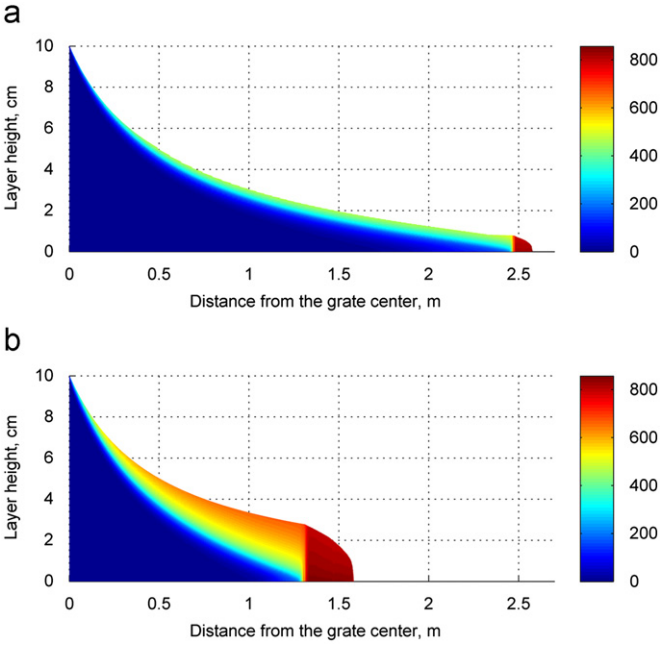

Fig. 7. Solid phase temperature profiles for fuels with (a) 70 wt% and (b) 40 wt% moisture content with primary air flow of 1 m^3/s.

1 m^3/s. Fig. 8 presents a comparison of the mean gas production rates for different primary air flows. The comparison shows that the mean combustion front propagation rate reaches its maximum when the air flow is 2 m^3/s. Higher air flows begin to cool the bed, resulting in a decrease in the propagation rates; especially carbon dioxide is produced less when the temperature has decreased below the critical point.

Moreover, air flows of 2 and 4 m^3/s cause oscillations in the gas production because they accelerate the combustion of the

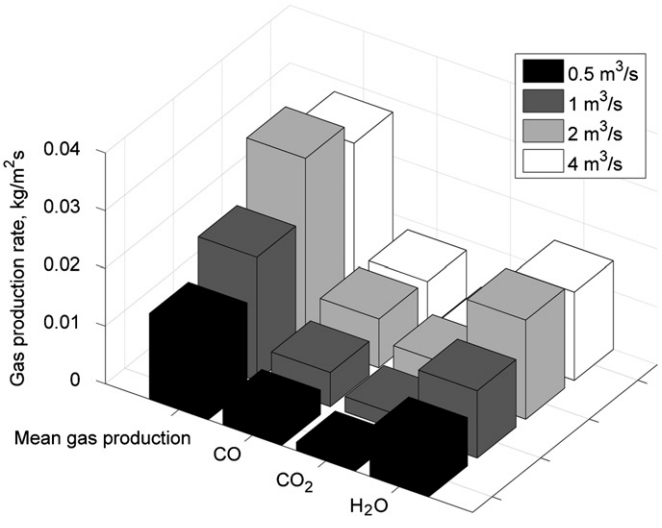

Fig. 8. Mean gas production rates for different primary air flows.

available char, as a result of which the char content is depleted and nothing happens until more char is formed in the pyrolysis reaction. In contrast, the flow of 1 m^3/s enables a steady char combustion rate without oscillations. In addition, the increased amount of oxygen supplied by larger air flows accelerates the combustion of the char. However, large airflows decrease the rate of the other reactions. These include the gasification reactions and the reactions taking place in the gas phase because they have high activation energies and are; therefore, limited by the decreased temperatures of the gas and the solid phases. In addition, simulations show that the larger the air flow, the more carbon monoxide is produced, whereas the release rate of carbon dioxide shows the opposite behavior: it decreases with increasing air flow. The reason for such behavior is that additional oxygen is consumed by char oxidation and no oxygen is left to oxidize CO to CO_2.

To conclude, the simulation results suggest that the char combustion reaction is diffusion limited, whereas the gasification and gas phase reactions are kinetically limited. Optimization of fuel combustion thus requires a compromise between char combustion and the other reactions by choosing an appropriate volumetric air flow. Particle size also affects the convective heat exchange because a bed with smaller particles provides a larger area for heat transfer. In addition, heat conduction inside the bed also depends on particle size because a bed with smaller particles has a larger area for absorbing the radiated energy. The next investigation is; therefore, on the effect of particle size on the combustion process.

5.3. Effect of particle size on biomass combustion

The simulation with different particle sizes was conducted using five different particle sizes: 50, 40, 30, 25, and 15 mm. Moisture content and airflow were fixed at 50 wt % and 1 m^3/s, respectively.

The simulation results show that the bed with the smallest particle size ignites most rapidly, for smaller particles absorb heat radiation energy more efficiently. The ignition delays are 23, 29, 37, 45, and 53 s for the particle diameters 15, 25, 30, 40, and 50 mm, respectively. Ignition time increases with particle size, and the largest particles take twice as long to ignite as those with the smallest diameter. However, smaller particles are more prone to cooling, and this effect is observed in the simulation results as temperature oscillations. The oscillations are the most significant in the case of particles measuring 15 mm. Chemical reactions heat the fuel layer, but as its temperature rises, the temperature gradient between the solid and gas phases become larger. As a result, the rate of heat transfer between these phases increases, resulting in oscillations. In contrast, large particles resist cooling more efficiently because they provide less surface for heat transfer than smaller particles do. Moreover, larger particles improve heat transfer inside the bed, enabling heat to spread more evenly in the bed, which causes much smaller temperature gradients in the bed. Consequently, improved heat transfer enhances the drying of the bed, but since the local temperatures of large particles are smaller than those of small particles, pyrolysis and char combustion take much longer. Table 2 shows the mean gas production rates for different particle sizes. Results show that as particle size is decreased by 10 mm the average combustion front propagation is increased by 2.5%, the largest propagation rate for particle diameter 15 mm reaches up to 0.0225 kg/(m^2s), while largest particle size, 50 mm, stays well below 0.02 kg/(m^2s).

5.4. Effect of gas recirculation on biomass fuel combustion

Gas recirculation is an important way of controlling the combustion efficiency and temperature of the furnace. It is, therefore, important to study how the recirculation specifically affects the combustion of fuel. In order to investigate the effect of recirculation on the burning behavior of biomass, the initial conditions of gas enthalpy and composition were changed. The

Table 2
Mean combustion front propagation rates for different particle sizes.

Particle diameter (mm)	Mean front propagation rate (kg/m^2 s)
15	0.0224
25	0.0218
30	0.0209
40	0.0202
50	0.0197

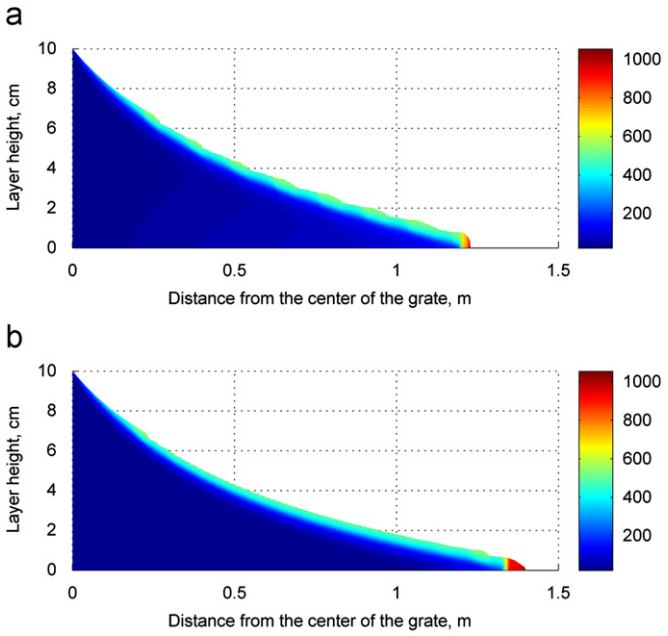

Fig. 9. Comparison of temperature profiles of fuel bed (a) with and (b) without recirculation.

following components were added to the initial conditions: 0.5 kg/m^3 of water steam, 0.5 kg/m^3 of CO and CO_2 each. The added components were assumed to have a temperature of 200 °C. Particle size and porosity were fixed at 35 mm and 0.5, respectively. To avoid oxygen deficiency, primary air flow was fixed at 2 m^3/s.

The obtained simulation results showed that the maximum temperatures of the fuel layer and the released gas indeed decreased to 900 and 2000 °C when recirculation was introduced. Prior to the introduction of gas recirculation, these were 1050 and 2700 °C, respectively. Despite the decreased maximal temperatures, the gas recirculation, nevertheless, accelerated the thermal conversion of fuel because the increased temperature of the gas flow enhanced the drying of the fuel, allowing the consequent reactions to start earlier. Fig. 9 compares the fuel temperature profiles of simulations with and without recirculation.

6. Conclusion

A one-dimensional model of a BioGrate furnace was developed to investigate the process phenomena in the furnace. The model was especially designed to study the effects of different operation conditions of a BioGrate furnace on biomass firing. The newest available reaction rate equations were utilized to describe char combustion and gasification with CO_2 and H_2O. The simulation results showed the significant dependence of the combustion process on moisture content: the moisture content significantly affected both the temperature of the gas and the solids. Lower moisture content permitted higher temperatures of the flue gas and fuel layer, allowing rapid combustion of fuel, whereas high moisture content delayed pyrolysis and char reactions, decreasing the overall conversion rate of fuel. The study of the effect of primary air flow suggested that low air flows induced oxygen deficiency in the combustion process, whereas larger flows cooled the fuel bed and decreased the overall combustion rate of fuel. Simulations with varying particle sizes revealed that small particles ignite quicker than large ones due to the ability of the small particles to absorb heat radiation more efficiently because of their large heat exchange area. In contrast, large particles absorbed radiation less efficiently, but they were less affected by convective heat transfer in the gas phase. This finding is supported by the investigation of Horttanainen et al. (2002) who noticed that a mixture of wood chips and saw dust burned better than when these fuels burned separately. Horttanainen et al. (2002) proposed that sawdust helped ignite the larger particles. The current simulation suggests that burning larger particles are less affected by gas flow, enabling the use of larger air flows, which accelerate fuel combustion. The study of flue gas recirculation proved the ability of recirculated flue gas to stabilize the combustion temperature, which prevents rapid temperature spikes in both the solid and gas phases. Recirculation also enhanced fuel combustion by heating the solid fuel. Further studies will study the validity of the developed model with data obtained from a BioGrate boiler furnace since pot furnace experiments are not fully able to describe the operation conditions of a boiler furnace. This is supported by a finding of Thunman and Leckner (2001), who noticed that fuel that burned in a boiler furnace with no problems could not be properly fired in a pot furnace.

Nomenclature

$\Delta H_{comb,C}$ reaction enthalpy of char combustion (J/kg)
ΔH_{evap} reaction enthalpy of drying (J/kg)
$\Delta H_{gasi,CO_2}$ reaction enthalpy of char gasification with carbon dioxide (J/kg)
$\Delta H_{gasi,H_2O}$ reaction enthalpy of char gasification with water steam (J/kg)
ΔH_{pyr} reaction enthalpy of pyrolysis (J/kg)
$C_{C_2H_2}$ concentration of acetylene (mol/cm^3)
C_{CO} concentration of carbon monoxide (mol/cm^3)
$C_{C_2H_4}$ concentration of ethylene (mol/cm^3)
C_{H_2} concentration of hydrogen (mol/cm^3)
C_{CH_4} concentration of methane (mol/cm^3)
C_{O_2} concentration of oxygen (mol/cm^3)
C_{H_2O} concentration of steam (mol/cm^3)
C_s the heat capacity of the solid phase (J/(kg K))
d_p particle diameter (m)
$e\sigma T_s^4$ energy flux out of the system (W/m^2)
h step size (m)
h_f enthalpy of the gas phase (J/kg)
I_{in} energy flux into the system (W/m^2)
$\Re$ gas constant (J/(mol K))
k_{cond} heat conduction coefficient of the solid phase (W/(m K))
k_{conv} heat convection coefficient between the gas and solid phases (W/(m^{2}K))
k_{fiber} heat conductivity of wood fiber (W/(m K))
k_g heat conductivity of the gas inside the wood pores (W/(m K))
k_e^0 effective heat conduction coefficient of the packed bed with no fluid flow (W/(m K))
k_g heat conduction coefficient of the fluid (W/(m K))
k_s heat conduction coefficient of the solid matter (W/(m K))
k_{rs} void-to-void heat conduction coefficient (W/(m K))
k_{rv} solid surface-to-solid surface heat conduction coefficient (W/(m K))
k_{min} minimal heat conduction coefficient (W/(m K))
k_{max} maximum heat transfer coefficient (W/(m K))
k_{n-1} value of the heat conductivity coefficient at x_{n-1} (W/(m K))
k_n value of the heat conductivity coefficient at x_n (W/(m K))
P_{CO_2} pressure of carbon dioxide (Pa)
P_{H_2O} pressure of water steam (Pa)
P_{O_2} pressure of oxygen (Pa)
Q_{n-1} energy flux leaving from point x_{n-1} towards x_n (W/m^2)
Q_n energy flux arriving at point x_n from x_{n-1} (W/m^2)
$R_{comb,C}$ reaction rate of char combustion (kg/(m^3 s))
R_{evap} reaction rate of drying (kg/(m^3 s))
R_f overall reaction rate of the solids (kg/(m^3 s))
R_{gasi,CO_2} reaction rate of char gasification with carbon dioxide (kg/(m^3 s))
R_{gasi,H_2O} reaction rates of char gasification with water steam (kg/(m^3 s))
R_{comb,H_2} oxidation rate of hydrogen (mol/(cm^3 s))
R_{comb,CH_4} oxidation rate of methane (mol/(cm^3 s))
R_{comb,C_2H_2} oxidation rate of acetylene (mol/(cm^3 s))
R_{comb,C_2H_4} oxidation rate of ethylene (mol/(cm^3 s))
$R_{comb,CO}$ oxidation rate of carbon monoxide (mol/(cm^3 s))
R_i rate of formation of gaseous component i (kg/(m^3 s))
R_{pyr} reaction rate of pyrolysis (kg/(m^3 s))
T_g temperature of the gas phase (K)
T_s temperature of the solid phase (K)
u discretized value of the temperature function (K)
v_f gas flow velocity (m/s)
v_p density number (m^{-1})
X degree of conversion of char
x vertical coordinate (m)
Y_i mass fraction of the gaseous component i
ε_b bed porosity

ρ_c	density of the char (kg/m^3)
ρ_{cel}	density of cellulose (kg/m^3)
ρ_{CO}	density of carbon monoxide (kg/m^3)
ρ_f	density of the gas phase (kg/m^3)
ρ_{H_2}	density of hydrogen (kg/m^3)
ρ_{Hemi}	density of hemicellulose (kg/m^3)
ρ_{O_2}	density of oxygen (kg/m^3)
ρ_{Water}	density of water (kg/m^3)
σ	Stefan–Boltzman constant (W/(m^2 K^4)

Acknowledgments

This work was partially supported by the Dynergia consortium project of the Finnish Funding Agency for Technology and Innovation (TEKES). The first author gratefully acknowledges the financial support by Finnish Graduate School in Chemical Engineering. The authors would like to recognize the comments and discussions provided by Dr. Juha Huotari and Dr. Jaakko Saastamoinen, whose contributions have been invaluable.

References

Alves, S.S., Figueiredo, J.L., 1989. A model for pyrolysis of wet wood. Chem. Eng. Sci. 44, 2861–2869.
Babushok, V.I., Dakdancha, A.N., 1993. Global kinetic parameters for high-temperature gas-phase reactions. Combust. Explosion Shock Waves 29, 464–489.
Bryden, K.M., Hagge, M.J., 2003. Modeling the combined impact of moisture and char shrinkage on the pyrolysis of a biomass particle. Fuel 82, 1633–1644.
Di Blasi, C., 1996. Heat, Momentum and Mass Transport Through a Shrinking Biomass Particle Exposed to Thermal Radiation. Chem. Eng. Sci. 5, 1121–1132.
Di Blasi, C., Branca, C., Sparano, S., La Mantia, B., 2003. Drying characteristics of wood cylinders for conditions pertinent to fixed-bed countercurrent gasification. Biomass Bioenergy 25, 45–58.
Di Blasi, C., 2009. Combustion and gasification rates of lignocellulosic chars. Prog. Energy Combust. Sci. 35, 121–140.
Dupont, C., Chen, L., Cances, J., Commandre, J.-M., Cuoci, A., Pierucci, S., Ranzi, E., 2009. Biomass pyrolysis: kinetic modeling and experimental validation under high temperature and flash heating rate conditions. J. Anal. Appl. Pyrol. 85, 260–267.
Ferziger, J.H., Peric, M., 2000. Computational Method for Fluid Dynamics, third ed. Springer-Verlag, Berlin, Heidelberg, New York.
Goh, Y.R., Yang, Y.B., Zakaria, R., Siddall, R.G., Nasserzadeh, V., Swithenbank, J., 2001. Development of an incinerator bed model for municipal solid waste incineration. Combust. Sci. Technol. 162, 37–58.
Horttanainen, M., Saastamoinen, J., Sarkomaa, P., 2002. Operational limits of ignition front propagation against airflow in packed beds of different wood fuels. Energy Fuels 16, 676–686.
Janssens, M., Douglas, B., 2004. Wood and Wood Products. In: Harper, C.A. (Ed.), Handbook of Building Materials for Fire Protection, McGraw-Hill, 542 pp.
Jämsä-Jounela, S.-L., 2007. Future trends in process automation. Annu. Rev. Control 31, 211–220.
Kær, S.K., 2005. Straw combustion on slow moving grates-a comparison of model predictions with experimental data. Biomass Bioenergy 28, 307–320.
Kiameh, P., 2002. Power Generation Handbook. McGraw-Hill.
Matsumoto, K., Takeno, K., Ichinose, T., Ogi, T., Nakanishi, M., 2009. Gasification reaction kinetics on biomass char obtained as a by-product of gasification in an entrained-flow gasifier with steam and oxygen at 900–1000 °C. Fuel 88, 519–527.
Peters, B., Bruch, C., 2001. A flexible and stable numerical method for simulating the thermal decomposition of wood particles. Chemosphere 42, 481–490.
Senneca, O., 2007. Kinetics of pyrolysis, combustion and gasification of three biomass fuels. Fuel Process. Technol. 88, 87–97.
Shin, D., Choi, S., 2000. The combustion of simulated waste particles in a fixed bed. Combust. Flame 121, 167–180.
Thunman, H., Leckner, B., 2001. Ignition and propagation of a reaction front in cross-current bed combustion of wet biofuels. Fuel 80, 473–481.
Thunman, H., Davidsson, K., Leckner, B., 2004. Separation of drying and devolatilization during conversion of solid fuels. Combust. Flame 137, 242–250.
Van der Lans, R.P., Pedersen, L.T., Jensen, A., Glarborg, P., Dam-Johansen, K., 2000. Modelling and experiments of straw combustion in a grate furnace. Biomass Bioenergy 19, 199–208.
W.W.W., Anon, MW Power Brochure, 〈http://www.mwpower.fi/mwpower/ru/mwpower_pages_ru.nsf/WebWID/WTB-090524-22575-77914/$File/Biopower_5_screen.pdf〉, 28.10.2011.
Yagi, S., Kunii, D., 1957. Studies on effective thermal conductivities in packed beds. A.I.Ch.E. J. 3, 373–381.
Yang, Y., Goh, B., Zakaria, Y.R., Nasserzadeh, R., Swithenbank, J., V., 2002. Mathematical modelling of MSW incineration on a traveling bed. Waste Manage. 22, 369–380.
Yang, Y.B., Yamauchi, H., Nasserzade, V., Swithenbank, J., 2003. Effects of fuel devolatilization on the combustion of wood chips and incineration of simulation municipal solid wastes in a packed bed. Fuel 82, 2205–2221.
Zhou, H., Jensen, A.D., Glaborg, P., Jensen, P.A., Kavaliauska, A., 2005. Numerical modeling of straw combustion in a fixed bed. Fuel 84, 389–403.